Catalysis Today 158 (2010) 22–28

Contents lists available at ScienceDirect

Catalysis Today

journal homepage: www.elsevier.com/locate/cattod

Iridium and ruthenium complexes covalently bonded to carbon surfaces by means of electrochemical oxidation of aromatic amines

Martina Sandroni[a], Giorgio Volpi[a], Jan Fiedler[b], Roberto Buscaino[c], Guido Viscardi[c], Luciano Milone[a], Roberto Gobetto[a], Carlo Nervi[a,*]

[a] Department of Chemistry IFM, University of Turin, via P. Giuria 7, 10125, Turin, Italy
[b] J. Heyrovský Institute of Physical Chemistry of the ASCR, v.v.i., Dolejškova 2155/3, 182 23, Prague, Czech Republic
[c] Department of General and Organic Chemistry, via P. Giuria 7, 10125 Turin, Italy

ARTICLE INFO

Article history:
Available online 31 July 2010

Keywords:
Functionalization
Glassy carbon electrode
Metallorganic complexes
Cyclic voltammetry

ABSTRACT

Bis(2-phenylpyridinate-C^2,N)-(4-(4-aminophenyl)-2,2′-bipyridine) iridium(III) hexafluorophosphate and bis(2,2′-bipyridine-N,N′)-(4-(4-aminophenyl)-2,2′-bipyridine) ruthenium(II) hexafluorophosphate were synthesized and characterized. In particular, electrochemical analyses showed irreversible amine-centred oxidations, which were exploited to functionalize a glassy carbon electrode. The functionalization was achieved by electrochemical oxidation of the amino group.

Surface modification was observed and studied via electrochemical techniques (cyclic voltammetry, square wave voltammetry).

The functionalization was performed at different potential values, and the effect of the collidine (2,4,6-trimethylpyridine) was evaluated. The surface coverage was assessed by integration of the peak current of the modified electrode signal. The formation of monolayers or multilayers depends on the oxidation potential used and on the presence of collidine in the functionalization cell.

1. Introduction

One of the challenges of chemistry in the near future is to achieve 100% selectivity of the desired product while maintaining an eco-compatible approach ("green chemistry") and develop renewable energy-based processes. Surface chemistry, nanosciences and catalysis are supposed to play key roles [1]. Recyclable catalysts can be produced by the immobilization of the active species on inorganic solid materials. Silica surface is a very well studied substrate and its functionalization is routinely performed [2,3]. One of the common strategies for attaching transition metal complexes on oxide surfaces usually takes place via metal–oxygen bond formation or via chemical vapour deposition of volatile organometallic species [4,5]. Silica and alumina (in all their forms) probably represent the most studied and employed support for catalysts. Much less attention has been paid to the synthesis of catalysts containing transition metals on non-oxide solids. Self-assembled monolayers (SAM) can be easily prepared on Au surface, but the Au–S bond is not very strong and not stable under oxidizing conditions. Gold nanoparticles have been inserted into pits of highly oriented pyrolytic graphite (HOPG) electrodes [6]. Carbon is a very interesting material (thanks also to its low cost), although usually cannot be employed in high temperature processes because it is oxidized, but it is used, for example, as support for low-temperature fuel cell electrocatalysis [7].

Stark and co-workers were able to synthesize in large scale air-stable nanoparticles having a nano-paramagnetic core and a carbon protective shell thick about 1 nm [8]. The latter can be functionalized on the surface, and the magnetic properties of the nanoparticles allow to fully recover them mechanically (by a magnet) after the reaction, in a fashion similar to the well known Merrifield solid state synthesis. The functionalization of such a nanoparticles [8] could lead to the production of catalysts that have the advantage and the properties of both the homogeneous and heterogeneous phases.

During last years we investigated the properties of new Os [9,10], Ru [11,12], Re [13–16] and Ir [17] organometallic complexes. The goal of the present communication is to show our results for the functionalization of carbon surfaces by means of organometallic moieties.

In the literature there are several examples of molecules covalently bonded on the electrode surface, but there are few cases that makes use of clean organometallic complexes. Carbon functionalization by means of strong covalent carbon–carbon bonds found new impetus after the work of Savéant and co-workers [18], who

* Corresponding author. Fax: +39 011 670 7855.
E-mail address: carlo.nervi@unito.it (C. Nervi).

0920-5861/$ – see front matter © 2010 Elsevier B.V. All rights reserved.
doi:10.1016/j.cattod.2010.06.025

used diazonium salts for facile electrochemical C–C bond formation. Another method is the oxidation of amine [19], which leads to the formation of a covalent C–N bond. Aliphatic amines has been thoroughly employed, by electrochemical [20] or spontaneous [21] oxidation, but less attention has been paid to the use of aromatic amines, due to their less (or no) reactivity. One of the aim of this job was to test the possibility to functionalize carbon surface by using organometallic complexes that contain ligands with aromatic amines.

2. Experimental

2.1. Reagents and chemicals

The reagents were purchased from Aldrich and used without further purification. Acetonitrile was distilled over calcium hydride just before use. Materials for electrochemistry were prepared as described elsewhere [22]. Tetrakis(2-phenylpyridinate-C^2,N)(μ-dichloro)di-iridium [23] and 4-(4-aminophenyl)-2,2′-bipyridine [24] were synthesized following the corresponding literature procedures.

2.2. Instrumentation

Electrochemistry was carried out in acetonitrile/0.1 M $TBAPF_6$, in the usual conditions [22] employing an Autolab PGSTAT302N electrochemical analyser controlled by a PC. Aqueous 3 M KCl calomel electrode (SCE) was used as reference electrode; half-wave potential of the ferrocene (Fc) standard couple (0/+1) was located at 0.386 V vs. SCE under our experimental conditions.

^1H and ^{13}C NMR spectra were registered with a Jeol EX 400 spectrometer (B_0 = 9.4 T, work frequency ^1H = 399.78 MHz) at 25 ± 0.5 °C. The solutions were prepared using acetone–d_6 and the spectra are referred to the non-deuterated solvent signal. The following abbreviations are used: s, singlet; d, doublet; t, triplet; m, multiplet. Mass spectra were recorder on a LCQ Advantage Max Thermo with ElectroSpray Ionization (ESI). In the spectra description the abbreviation M was used for the molecular ion. The reported values are in atomic mass units. The UV–vis spectra were registered using a double beam Perkin Elmer spectrophotometer mod. LAMBDA 20, equipped with a deuterium lamp as UV source and a tungsten lamp as vis source. The spectra were performed in acetonitrile. The wavelength of the absorption maxima is reported in nm, and the molar absorption coefficients (ε) are in l cm^{-1} mol^{-1}. Emission spectra and luminescence lifetime were determined following the methods previously reported [17].

2.3. Synthesis and chacterization of bis(2-phenylpyridinate-C^2,N)-(4-(4-aminophenyl)-2,2′-bipyridine) iridium(III) hexafluorophosphate (**1**)

Tetrakis(2-phenylpyridinate-C^2,N)(μ-dichloro)di-Iridium (100 mg, 0.09 mmol) and 4-(4-aminophenyl)-2,2′-bipyridine (67 mg, 0.27 mmol) were added to 20 ml of a 1:1 mixture of dichloromethane and methanol. The solution was degassed and heated to reflux under inert atmosphere for 2 h, then allowed to cool to room temperature and concentrated to half volume under reduced pressure. The precipitate was removed by centrifugation. A few drops of a saturated NH_4PF_6 aqueous solution were added to the remaining solution, and the precipitate was collected and washed with diethyl ether (2× 5 ml), then dried under vacuum. The product (91 mg) was purified by chromatography on silica gel (CH_2Cl_2:CH_3OH = 90:10) and yielded a yellow-beige solid (46 mg, 28%).

^1H NMR (400 MHz, acetone–d_6): δ (ppm) = 9.08 (d, 1H, J = 8.4 Hz), 8.98 (s, 1H), 8.22–8.32 (m, 3H), 8.11 (d, 1H, J = 5.4 Hz), 7.88–7.96 (m, 6H), 7.78–7.87 (m, 4H), 7.70 (t, 1H, J = 6.5 Hz), 7.17 (m, 2H), 7.04 (m, 2H), 6.92 (m, 2H), 6.84 (d, 2H, J = 9.8 Hz), 6.37 (d, 1H, J = 4.0 Hz), 6.35 (d, 1H, J = 4.1 Hz), 5.42 (s, 2H). ^{13}C NMR (100 MHz, acetone–d_6): δ (ppm) = 168.81, 168.63, 152.65, 152.05, 151.87, 151.61, 151.37, 151.31, 150.67, 150.44, 149.79, 149.64, 145.07, 144.92, 140.27, 139.76, 139.17, 139.13, 133.13, 131.97, 131.40, 131.06, 129.88, 129.16, 126.25, 126.12, 125.53, 124.62, 124.53, 123.80, 123.26, 123.19, 120.75, 115.62, 115.10, 115.04. MS (ESI^+): m/z = 748 (100%, $(M\text{-}PF_6)^+$). UV–vis (CH_3CN): 255 nm (43,000 l cm^{-1} mol^{-1}), 335 nm (23,000 l cm^{-1} mol^{-1}), 375 nm (21,000 l cm^{-1} mol^{-1}). Emission (CH_3CN, λ_{exc} = 375 nm): 593 nm, Φ = 0.005, τ = 800 ns.

2.4. Synthesis and characterization of bis(2,2′-bipyridine-N,N′)-(4-(4-aminophenyl)-2,2′-bipyridine) ruthenium(II) hexafluorophosphate (**2**)

Bis(2,2′-bipyridine-N,N′)dichloro ruthenium(II) (148 mg, 0.31 mmol) and 4-(4-aminophenyl)-2,2′-bipyridine (90 mg, 0.36 mmol) were added to 30 ml of ethylene glycol. The mixture was degassed and heated to reflux under inert atmosphere for 4 h. Water (10 ml) was added and the complex was precipitated by adding a few drops of a saturated NH_4PF_6 aqueous solution. The red solid (180 mg) was filtered and washed with a few ml of water. The product was purified by flash chromatography on silica gel (CH_3CN:H_2O = 90:10 → CH_3CN:H_2O sat KPF_6 = 90:10) yielding a red solid (87 mg, 30%).

^1H NMR (400 MHz, acetone–d_6): δ (ppm) = 8.98 (d, 1H, J = 8.2 Hz), 8.92 (s, 1H), 8.75 (d, 4H, J = 8.2 Hz), 8.14 (m, 7H), 8.00 (m, 4H), 7.78 (m, 3H), 7.71 (d, 1H, J = 6.2 Hz), 7.55 (m, 4H), 6.81 (d, 2H, J = 9.1 Hz), 5.29 (s, 2H). ^{13}C NMR (100 MHz, acetone–d_6): δ (ppm) = 157.99, 157.65, 157.50, 152.09, 152.03, 151.99, 151.94, 151.45, 150.02, 138.33, 128.81, 128.26, 128.08, 124.84, 124.77, 123.19, 122.79, 119.96, 115.02. MS (ESI^+): m/z = 806 (96%, $(M\text{-}PF_6)^+$), 331 (100%, $(M\text{-}2\ PF_6)^{2+}$). UV–vis (CH_3CN): 244 nm (87,000 l cm^{-1} mol^{-1}), 288 nm (212,000 l cm^{-1} mol^{-1}), 344 nm (60,100 l cm^{-1} mol^{-1}), 458 nm (54,700 l cm^{-1} mol^{-1}). Emission (CH_3CN, λ_{exc} = 458 nm): 628 nm, Φ = 0.020, τ = 950 ns.

2.5. General procedure for electrode functionalization

Before every experiment the working electrode, a glassy carbon of 2 mm diameter, was polished on alumina nanopowder suspension in deionized water, and rinsed with water and acetone. The blank signal was registered in a solution containing only the supporting electrolyte.

The functionalization was accomplished by cyclic voltammetry (scan rate 200 mV/s, 10 scans in a 1 mM solution of complex) in acetonitrile solutions using $TBAPF_6$ 0.1 M as supporting electrolyte. The switching potentials was selected to be slightly more positive than the oxidation peak of the amino group. Functionalization was carried out also at other potentials if more oxidation peaks were present. Surface modification caused current intensity decrease at every cycle. The experiments were repeated in a solution containing collidine (2,4,6-trimethylpyridine), which helps the functionalization by favouring the cation radical deprotonation [25].

After each functionalization cycle the electrode was rinsed with acetone and sonicated for 5 min in distilled acetonitrile, to remove any physisorbed molecules (carbon is sometimes subjected to adsorption phenomena [26]). The presence of the covalently bound complexes was evaluated electrochemically in a solution containing the supporting electrolyte only, which generates reversible redox signals characteristic of the species. After each functionalization cycle (10 CV scans) two CV and one SWV were performed to verify the modification of the electrode.

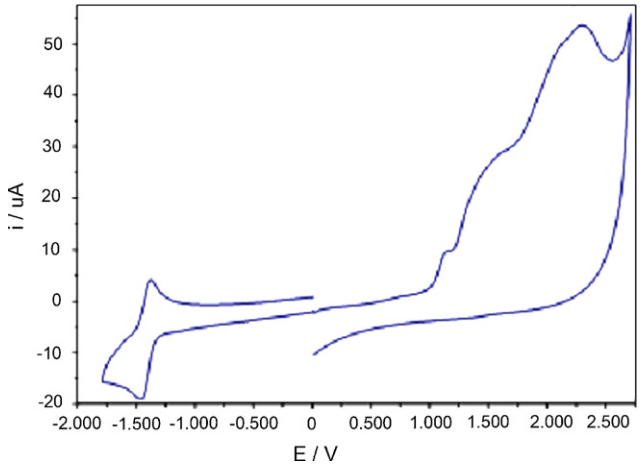

Fig. 1. CV of complex **1** in MeCN solution, scan rate 200 mV/s, GC electrode.

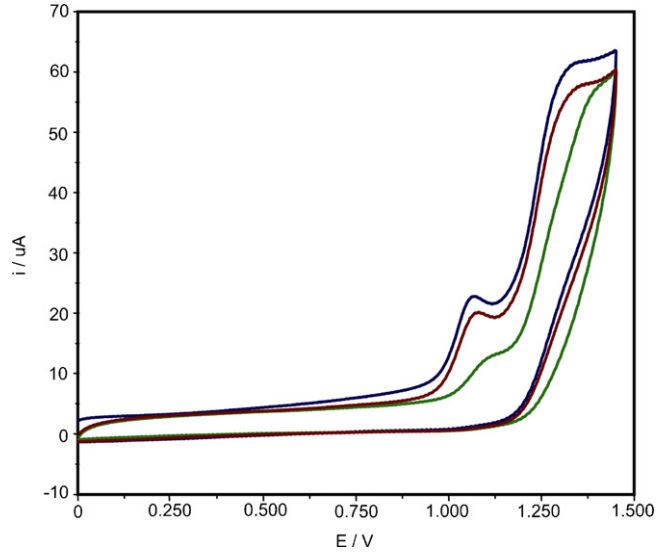

Fig. 2. Current intensity decrease observed during functionalization cycles with a solution 1.053 mM of **1** in CH_3CN/0.1 M $TBAPF_6$. Depicted first, second and third CV scan at 200 mV/s.

2.6. Surface coverage

The surface coverage (Γ) is a measure of the number of molecules bound to the surface. It can be assessed [19,27] by means of the formula $\Gamma = Q/FA$, where F is the Faraday constant, A is the apparent area of the electrode and Q is the charge that reduces or oxidize the organometallic complexes covalently bonded on the electrode surface. Q was evaluated by integration of the background-corrected CV peak [19]. For a monolayer, the theoretical value of Γ can be computed knowing the surface area of each molecule, the latter estimated from quantum mechanical calculation [27]. The surface coverage of a simple organic molecule like substituted benzene is about 10^{-9} mol cm^{-2} [20]. Quick DFT calculation performed on complex **1** (after geometry optimization at B3LYP/3-21G level) roughly estimate its molecular surface to be 100 Å^2. Similar value can be computed for complex **2**. This is approximately 10 times bigger than the molecular surface of a para-benzene substituted molecule [20]. Therefore a value of $\Gamma \cong 10^{-10}$ mol cm^{-2} is expected for a monolayer of our organometallic derivatives. It must be taken into account that the experimental surface coverage value is probably overestimated, because the surface is not completely smooth as it is implicitly assumed while considering the apparent area of the electrode. The actual area of the polished glassy carbon electrode was assessed by means of chronoamperometry. 1.075 mM ferrocene in acetonitrile/0.1 M $TBAPF_6$ was used as a standard solution. The actual area turn out about 34% higher than the geometrical area of the used disc electrode. The corrected value $A = 4.21 \times 10^{-2}$ cm^2 was assumed throughout all the measurements.

3. Results and discussion

3.1. Functionalization with the complex *1*

The electrochemical behaviour of the iridium complex **1** is similar to that of the analogues Ir cyclometalated phenylpyridine derivatives [17], but the presence of the amino group introduces an extra chemically irreversible oxidation. CV of **1** in acetonitrile solution (Fig. 1), using $TBAPF_6$ as supporting electrolyte and at a scan rate of 200 mV/s, shows three irreversible oxidations (E_p = +1.11, +1.48 and +2.29 V vs. SCE) and one reversible reduction ($E_{1/2}$ = −1.43). A second irreversible reduction process was detected at E_p = −2.06 V vs. SCE.

The reversible reduction at −1.43 V, commonly considered metal-centred [17], was chosen as probe to verify the presence of the complex bound to the electrode surface (see below). Its value is not altered by the modification of the electrode surface, indicating that the metal centre is almost not affected by the functionalization process. On the other hand, it should be mentioned that the oxidations are intimately related with the functionalization process, hence the values of peak potentials herein reported are influenced by the non-innocent behaviour of the electrode material.

3.1.1. Functionalization without collidine

The functionalization experiments were performed at three different oxidation potentials (+1.15 V, +1.45 V and +1.70 V vs. SCE) with the aim to evaluate the effect of the oxidation potential on surface modification. Fig. 2 reports the first three consecutive CV scans for a solution containing complex **1**. After the third scan

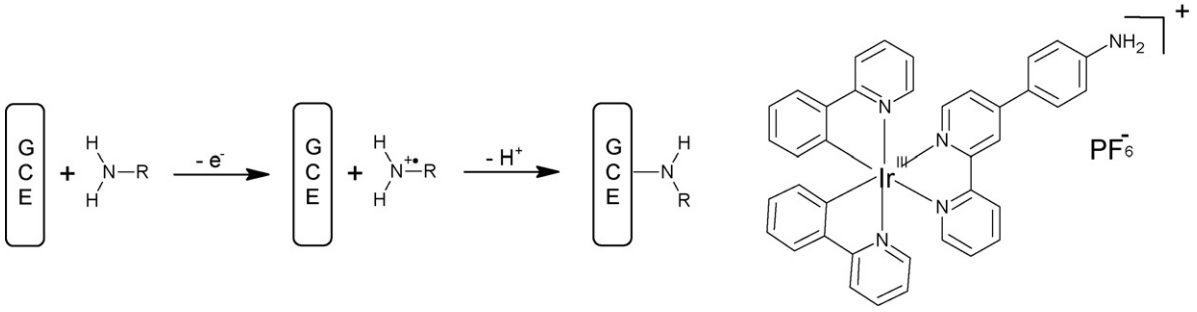

Fig. 3. Mechanism of the glassy carbon electrode functionalization by oxidation of the amine function of compound **1**.

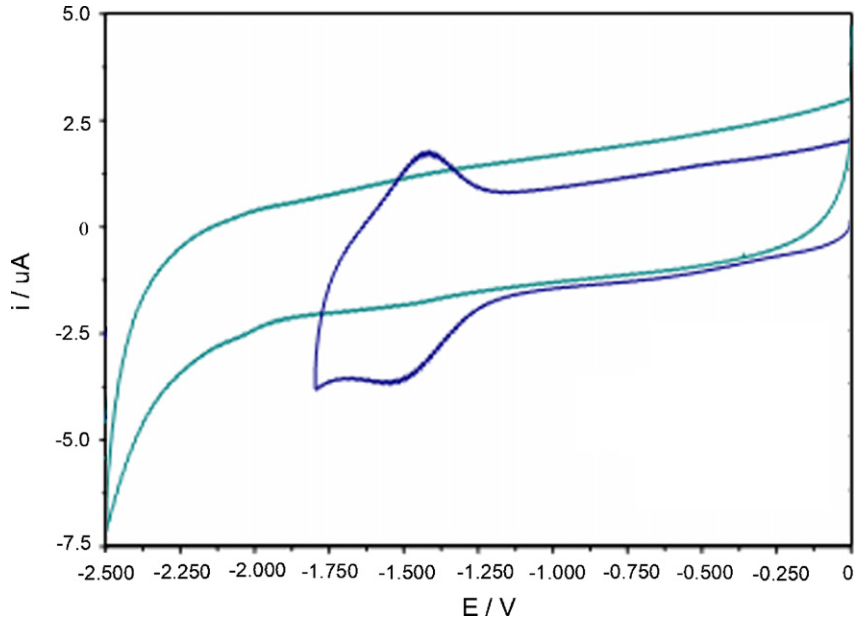

Fig. 4. CV at 200 mV/s (reduction scan) in clean MeCN/0.1 M $TBAPF_6$ solution of polished (background) and functionalized ( ) GC electrode.

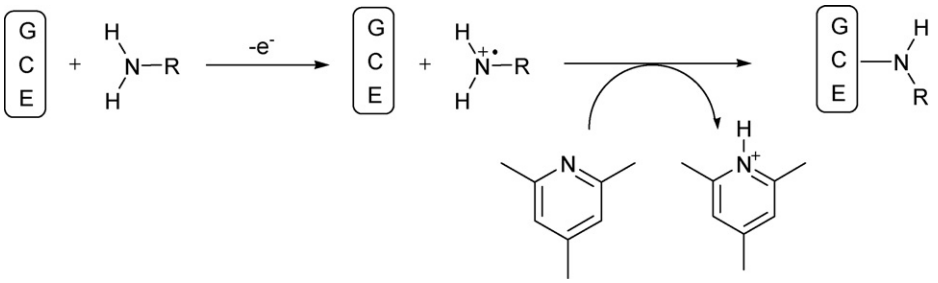

Fig. 5. Mechanism of the GCE functionalization in the presence of collidine, which deprotonates the radical cation.

the oxidation peak at about E_{pa} = +1.11 V reduces significantly. The functionalization procedure (series of 10 CV scans) was repeated seven times, which turn out to be enough to reach steady-state conditions (unchanging CV).

The irreversible oxidation peak at +1.11 V is assigned to the oxidation of amine, which in turn undergoes a chemical reaction on the electrode surface with the formation of a covalent C–N bond. The mechanism [20] is summarized in Fig. 3. The progressive surface coverage reduces the available electrode area, thus accounting for the observed decrease of current intensity in CV experiments.

The maximum degree of coverage was reached already during the first cycle of the functionalization experiment. In fact, the intensity of the reversible reduction peak at −1.43 V (see Fig. 4), recorded with the modified electrode in a new clean solution containing only the supporting electrolyte, did not increase after the subsequent cycles. The surface coverage of 2.6×10^{-10} mol cm^{-2} is compatible with the presence of a monolayer.

The functionalization obtained at higher oxidation potentials did not lead to a plateau after the first cycle; the reduction signal obtained with the modified electrode continued to increase at every cycle. The surface coverage started from a value of 3.7×10^{-9} mol cm^{-2} for the first cycle of functionalization at the second peak, and increases after every cycle. This value is compatible with the formation of a multilayer.

The second oxidation, metal-centred, clearly favour the formation of multilayers. This is not surprising considering that an intramolecular electron transfer can occur between the oxidized metal and the amine function [25]. More simply, when the com-

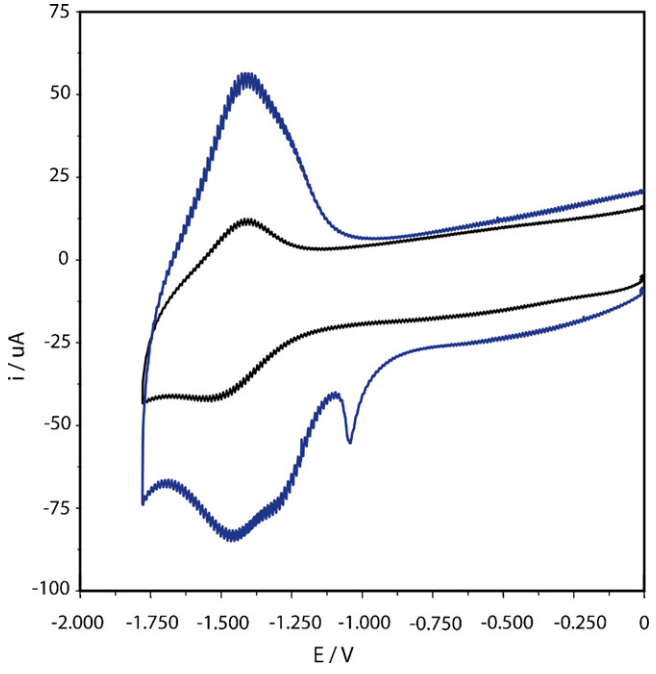

Fig. 6. Comparison between the signal of the electrode modified at the first oxidation wave with ( ) and without ( ) collidine.

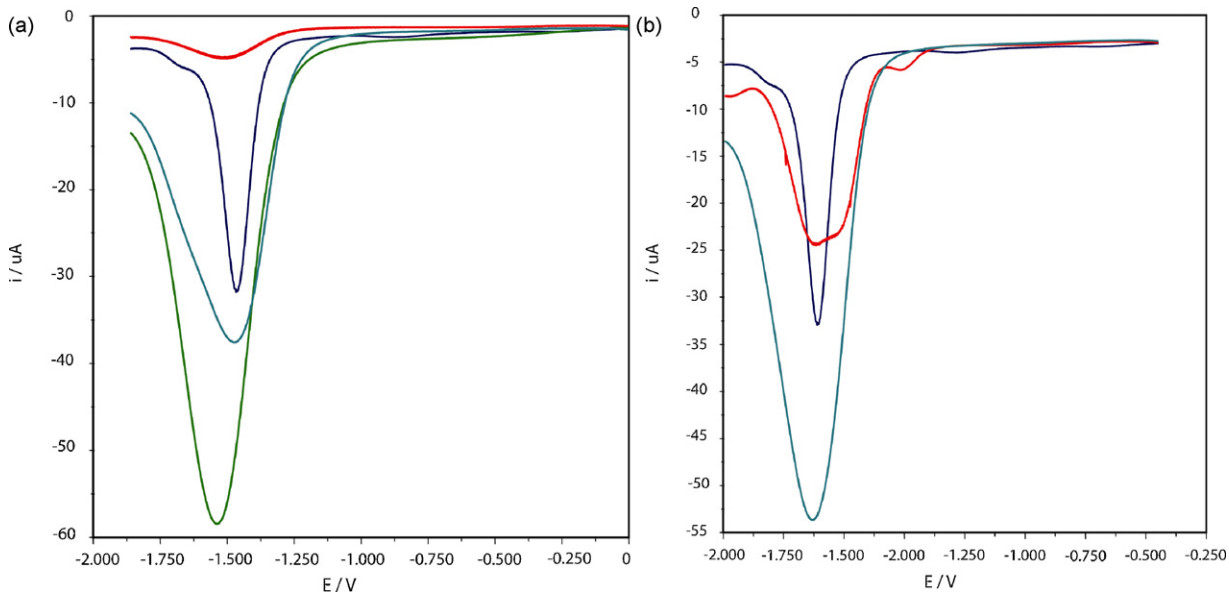

Fig. 7. Comparison between the SWV peaks of the complex **1** in solution ( ) and on the modified electrode (a- no collidine; b- presence of collidine). Functionalization potential = +1.15 V vs. SCE ( ); +1.45 V vs. SCE ( ); +1.70 V vs. SCE ( ).

plex **1**, already covalently bonded to the surface, undergoes the reversible metal-centred oxidation, it is able to oxidize a second non-bonded molecule of **1**, which results in the formation of multilayers. The plateau was reached after 9 cycles (90 total CV scans) during the functionalization at +1.70 V vs. SCE (third wave).

3.1.2. Functionalization with collidine

The use of collidine [25] (Fig. 5) facilitates the mechanism outlined in Fig. 3.

The functionalization was carried out by means of 4 cycles of 10 scans each. 15 μl of collidine was added into the electrochemical cell. A general increase in surface coverage and modification speed was observed. The main difference could be noticed during the functionalization at the first oxidation wave: the modified electrode signal in fact grew after every cycle, and did not reach a plateau after the first one. Observing the shape of the CV reduction wave (Fig. 6) appears a second peak at a slightly less negative potential, which is probably due to the formation of multilayer.

The results obtained at the second and the third oxidation wave follow the same trend, but the relative increase of the functional-

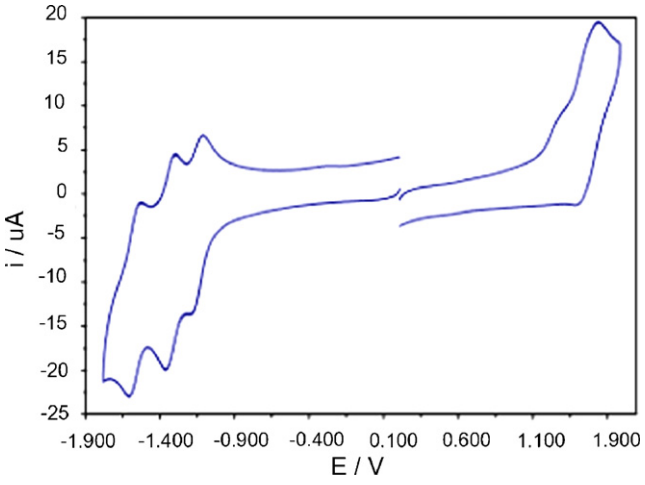

Fig. 9. CV of complex **2** in MeCN solution, scan rate 200 mV/s, GC electrode.

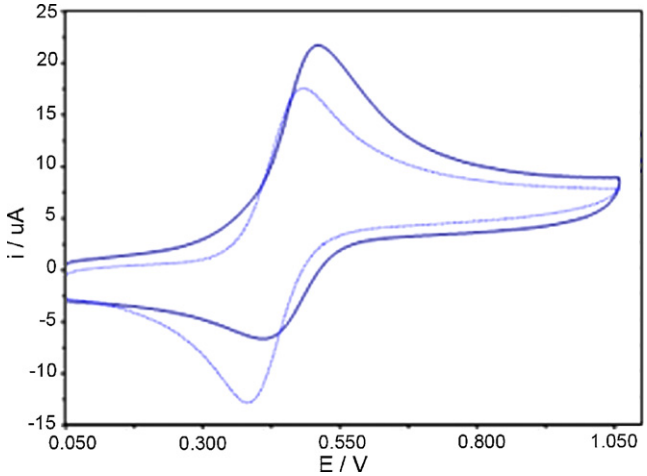

Fig. 8. Comparison of the ferrocene (Fc/Fc^+) peak, obtained with clean ( ) and modified ( ) GC electrode.

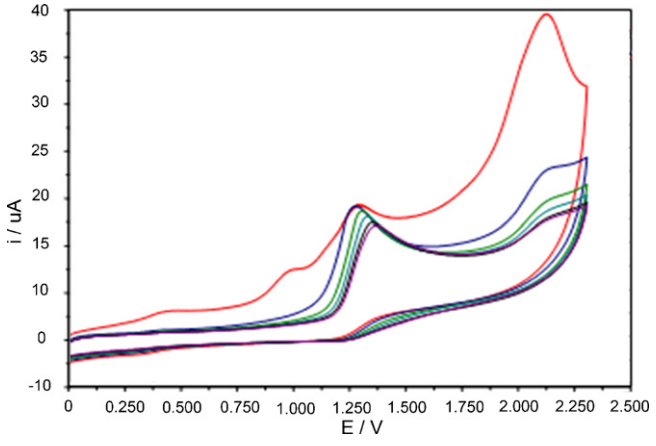

Fig. 10. CV changes observed during functionalization cycles with a solution 0.884 mM of **2** containing 15 μL of collidine, in CH_3CN/0.1 M $TBAPF_6$. Depicted first (largest current response) to seventh CV scan at 200 mV/s.

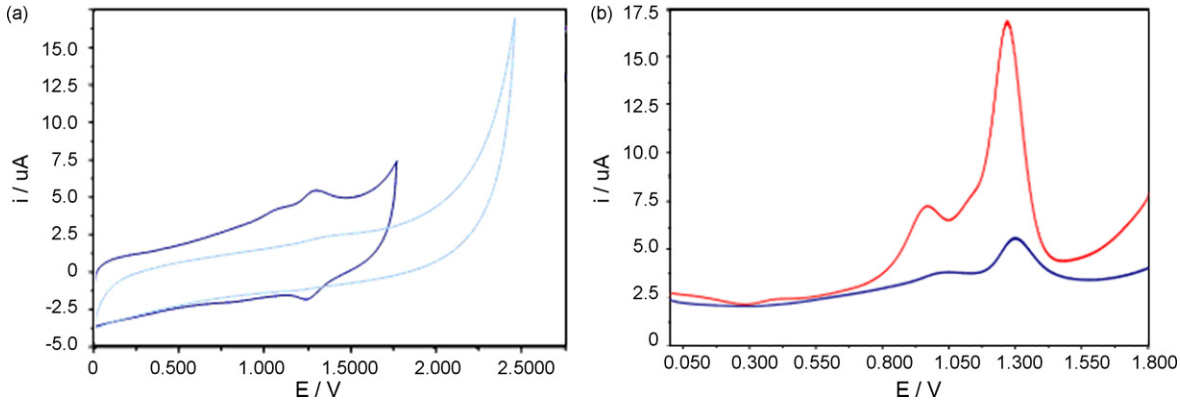

Fig. 11. (a) Comparison between the background ( ) and the CV signal obtained with the functionalized electrode ( ) and (b) Comparison between the SWV signal of the complex in solution ( ) and that of the functionalized electrode in a clean electrochemical cell ( ).

ization efficiency is less pronounced. Considering all the surface modification experiments (different functionalization potentials, presence of collidine or not), it is noteworthy that, in nearly every case, the intensity of the SWV peak of the bound complex on the glassy carbon electrode could equal or exceed that of the complex in solution (Fig. 7). Only the functionalization at the first oxidation wave without collidine, which probably led to the formation of a monolayer, gave a less intense signal than that of the free complex. The little difference between the nitrogen- and metal-centred oxidations makes the differences between the formation of a mono- or multilayer. The collidine facilitate the mechanism of hydrogen abstraction with the result that a multilayer is obtained.

The calculated surface coverage is respectively 1.2×10^{-9} and 2.1×10^{-9} mol cm^{-2} for the functionalization at the first and at the second peak with collidine. It should be noticed that the complex solution undergoes degradation after some days in presence of collidine.

3.1.3. CV of ferrocene on the modified electrode

The CV of a ferrocene solution in acetonitrile (Fig. 8) was done with the same GC electrode, before and after functionalization. The shape of the oxidation peak changed if the scan was performed with the modified electrode: the forward current intensity increased while the backward intensity decreased. The first phenomenon could be due to preferential interactions between the neutral ferrocene and the aromatic systems of the ligands (that probably lead to adsorption on the surface by π–π stacking); the backward peak decrease could be attributed to the electrostatic repulsion between the positive ferrocinium and the bound complex, positively charged. The oxidation potential is shifted to more positive potentials. This behaviour is typical of modified electrodes.

3.2. Functionalization with the complex ***2***

The cyclic voltammogram of the ruthenium complex **2**, performed in acetonitrile/TBAPF$_6$ 0.1 M and at a scan rate of 200 mV/s, shows two oxidations at E_p = +1.14 V and $E_{1/2}$ = +1.25 V vs. SCE, the first irreversible and the second partially reversible (Fig. 9). There are also reversible reductions at $E_{1/2}$ = −1.35 V, $E_{1/2}$ = −1.53 V, $E_{1/2}$ = −1.77 V and an irreversible process at rather negative potentials (E_p = −2.40 V vs. SCE).

The electrochemistry of ruthenium polypyridine complexes is well known. The partially reversible oxidation process is ruthenium-centred (Ru^{II}/Ru^{III}), while the three reversible reductions are mainly centred on the ligand. The shoulder at +1.14 V is probably due to the amine oxidation: a similar peak was in fact observed during the characterization of the free ligand.

The ruthenium reversible oxidation wave was chosen as a diagnostic peak to verify the presence of the complex bound to the carbon surface.

3.2.1. Functionalization without collidine

After 10 CV scans between 0 and 1.8 V (vs. SCE) no current decrease was observed, and no signals of electrode modifications were recorded. The different behaviour with respect to complex **1** cannot be easily explained. Probably the electronic properties of the two complexes could give some hints about the different behaviour.

3.2.2. Functionalization with collidine

15 μl of collidine was added into the electrochemical cell. The functionalization was at first tried with a series of CV scans from 0 V to 1.5 V vs. SCE, but the small current decrease suggested no or little surface modification. A scan up to 2.3 V, a very positive potential, showed the presence of a new irreversible oxidation peak at 2.1 V (Fig. 10). Seven scans up to 2.3 V were then performed, during which a remarkable current was observed. During these scans the peak at 1.29 V shifted towards more positive values.

After the treatment, the electrode was sonicated in acetonitrile and transferred to a clean solution containing the supporting electrolyte only. The CV showed a reversible peak at 1.28 V vs. SCE (ΔE_p = 63 mV), assigned to ruthenium oxidation (Ru^{II}/Ru^{III}). A qualitative comparison between the complex in solution was accomplished through a square wave voltammetry scan (Fig. 11): the signal obtained with the functionalized electrode is 1/6 of the free complex signal.

The surface coverage obtained by integration of the reversible oxidation peak is 3.43×10^{-10} mol cm^{-2}, which is compatible with the presence of a monolayer.

4. Conclusions

The aim of the work was the synthesis of iridium and ruthenium complexes, with suitable properties for electrode functionalization, and to demonstrate that in this cases the electrochemical oxidation of aromatic amines leads to carbon electrode modification. With regard to this, 4-(4-aminophenyl)-2,2′-bipyridine was chosen because of the chelating properties of the bipyridine moiety and the presence of an oxidizable amino group that can be used for direct electrochemical functionalization or converted into diazonium salts. The synthesized complexes were thoroughly characterized, with particular attention to the electrochemical properties.

Complexes **1** and **2** were used to carry out functionalization experiments on a glassy carbon electrode, via electrochemical techniques. The complex grafting was obtained by a series of CV cycles, according to a mechanism which has been examined in depth for

aliphatic amines, but was first reported in the last years for aromatic amines, and in particular for amine containing metallorganic complexes. The modified electrode was studied with electrochemical techniques (CV and SWV), which allowed to estimate the surface coverage.

The influence of different factors on functionalization was evaluated during this work. The oxidation potential applied during the grafting scans is an important parameter since it affects the surface modification mechanism. In general a more positive potential leads to an increase of the surface coverage, but does not guarantee the formation of a single monolayer. The presence of collidine (2,4,6-trimethylpyridine) increases the coverage because it scavenges the protons, which are formed upon grafting. In the case of complex **2** it was the only way to promote its grafting, but for complex **1** very probably promotes also the formation of multilayer.

Acknowledgements

The authors thank European COST project No D36/001/06, Regione Piemonte (Italy), and GACR (grant 203/09/0705) for financial support.

References

[1] G.A. Somorjai, H. Frei, J.Y. Park, J. Am. Chem. Soc. 131 (2009)16589.
[2] K. Motokura, M. Tada, Y. Iwasawa, Catal. Today 147 (2009) 203.
[3] K. Motokura, S. Tanaka, M. Tada, Y. Iwasawa, Chem. Eur. J. 15 (2009)10871.
[4] M. Tada, Y. Iwasawa, Chem. Commun. (2006) 2833.
[5] R. Psaro, S. Recchia, Catal. Today 41 (1998) 139.
[6] M. Limat, G. Foti, M. Hugentobler, R. Stephan, W. Harbich, Catal. Today 146 (2009) 378.
[7] E. Antolini, Appl. Catal. B: Environ. 88 (2009) 1.
[8] R.N. Grass, E.K. Athanassiou, W.J. Stark, Angew. Chem. Int. Ed. 46 (2007) 4909.
[9] C. Garino, S. Ghiani, R. Gobetto, C. Nervi, L. Salassa, V. Ancarani, P. Neyroz, L. Franklin, J.B.A. Ross, E. Seibert, Inorg. Chem. 44 (2005) 3875.
[10] R. Gobetto, C. Nervi, B. Romanin, L. Salassa, M. Milanesio, G. Croce, Organometallics 22 (2003) 4012.
[11] R. Gobetto, G. Caputo, C. Garino, S. Ghiani, C. Nervi, L. Salassa, E. Rosenberg, J.B.A. Ross, G. Viscardi, G. Martra, I. Miletto, M. Milanesio, Eur. J. Inorg. Chem. (2006) 2839.
[12] C. Garino, R. Gobetto, C. Nervi, L. Salassa, E. Rosenberg, J.B.A. Ross, X. Chu, K.I. Hardcastle, C. Sabatini, Inorg. Chem. 46 (2007) 8752.
[13] A. Albertino, C. Garino, S. Ghiani, R. Gobetto, C. Nervi, L. Salassa, E. Rosenberg, A. Sharmin, G. Viscardi, R. Buscaino, G. Croce, M. Milanesio, J. Organomet. Chem. 692 (2007) 1377.
[14] L. Salassa, C. Garino, A. Albertino, G. Volpi, C. Nervi, R. Gobetto, K.I. Hardcastle, Organometallics 27 (2008) 1427.
[15] C. Garino, T. Ruiu, L. Salassa, A. Albertino, G. Volpi, C. Nervi, R. Gobetto, K.I. Hardcastle, Eur. J. Inorg. Chem. (2008) 3587.
[16] C. Garino, S. Ghiani, R. Gobetto, C. Nervi, L. Salassa, G. Croce, M. Milanesio, E. Rosenberg, J.B.A. Ross, Eur. J. Inorg. Chem. (2006) 2885.
[17] G. Volpi, C. Garino, L. Salassa, J. Fiedler, K.I. Hardcastle, R. Gobetto, C. Nervi, Chem. Eur. J. 15 (2009) 6415.
[18] P. Allongue, M. Delamar, B. Desbat, O. Fagebaume, R. Hitmi, J. Pinson, J.M. Saveant, J. Am. Chem. Soc. 119 (1997) 201.
[19] B. Barbier, J. Pinson, G. Desarmot, M. Sanchez, J. Electrochem. Soc. 137 (1990) 1757.
[20] A. Adenier, M.M. Chehimi, I. Gallardo, J. Pinson, N. Vila, Langmuir 20 (2004) 8243.
[21] A. Adenier, N. Barre, E. Cabet-Deliry, A. Chausse, S. Griveau, F. Mercier, J. Pinson, C. Vautrin-Ul, Surf. Sci. 600 (2006) 4801.
[22] E. Rosenberg, M.J. Abedin, D. Rokhsana, D. Osella, L. Milone, C. Nervi, J. Fiedler, Inorg. Chim. Acta 300 (2000) 769.
[23] S. Sprouse, K.A. King, P.J. Spellane, R.J. Watts, J. Am. Chem. Soc. 106 (1984) 6647.
[24] O. Johansson, M. Borgstrom, R. Lomoth, M. Palmblad, J. Bergquist, L. Hammarstrom, L.C. Sun, B. Akermark, Inorg. Chem. 42 (2003)2908.
[25] O. Buriez, E. Labbé, P. Pigeon, G. Jaouen, C. Amatore, J. Electroanal. Chem. 619–620 (2008) 169.
[26] R.L. McCreery, Chem. Rev. 108 (2008) 2646.
[27] Y.C. Liu, R.L. McCreery, J. Am. Chem. Soc. 117 (1995) 11254.